Highly Ductile Polypropylene Based Ternary Blends for High Voltage Insulation

Citation for the original published paper (version of record):
Sowinski, P., Xu, X., Gkourmpis, T. et al (2025). Highly Ductile Polypropylene Based Ternary Blends for High Voltage Insulation. Journal of Applied Polymer Science, 142(22).
http://dx.doi.org/10.1002/app.56955

Journal of Applied Polymer Science

WILEY

Applied Polymer SCIENCE

RESEARCH ARTICLE OPEN ACCESS

Highly Ductile Polypropylene Based Ternary Blends for High Voltage Insulation

Przemyslaw Sowinski[1] | Xiangdong Xu[2] | Thomas Gkourmpis[3] | Per-Ola Hagstrand[3] | Christian Müller[1]

[1]Department of Chemistry and Chemical Engineering, Chalmers University of Technology, Göteborg, Sweden | [2]Department of Electrical Engineering, Chalmers University of Technology, Göteborg, Sweden | [3]Innovation & Technology, Borealis AB, Stenungsund, Sweden

Correspondence: Przemyslaw Sowinski (sowinski@chalmers.se) | Per-Ola Hagstrand (per-ola.hagstrand@borealisgroup.com) | Christian Müller (christian.muller@chalmers.se)

Received: 7 December 2024 | **Revised:** 17 February 2025 | **Accepted:** 19 February 2025

Funding: This work was supported by Borealis.

Keywords: dielectric properties | insulation materials | polyolefin blends | structure–property relationships | thermoplastics

ABSTRACT

High voltage insulation materials must combine excellent dielectric and thermomechanical properties. Ternary blends based on isotactic polypropylene (PP) tend to feature a low electrical conductivity and high melting temperature but are usually characterized by a too low ductility. Here, it is shown that the cooling rate can be used to significantly improve the ductility without compromising the otherwise excellent property portfolio. Rapid cooling of ternary blends comprising PP, low-density polyethylene (LDPE) and a polystyrene-*b*-(ethylene-*co*-butylene)-*b*-polystyrene (SEBS) elastomer is found to result in a material with an elongation at break above 500%, which is maintained even after prolonged annealing at up to 135°C. At the same time, the ternary blend continues to exhibit a high elastic modulus above the melting temperature of LDPE and a low direct-current (DC) electrical conductivity of $0.7 \times 10^{-15}\,\mathrm{S\,m^{-1}}$ at 70°C and an electric field of $30\,\mathrm{kV\,mm^{-1}}$. Evidently, rapid cooling of PP-based insulation materials can facilitate the preparation of highly ductile insulation materials.

1 | Introduction

The share of electricity produced from renewable sources of energy is rapidly increasing. In contrast to conventional power plants, wind and solar farms, as well as hydroelectric dams, tend to be located at a considerable distance from cities where most electricity is consumed. High-voltage direct-current (HVDC) systems are ideally suited for transporting electricity over long distances with minimal losses [1]. HVDC cables require an insulation layer so that they can be laid on the bottom of the sea or buried underground. The most advanced type of cable insulation is composed of an extruded insulation layer. Today, low-density polyethylene (LDPE) is commonly used, which must be crosslinked to improve the form stability at elevated temperatures, resulting in crosslinked polyethylene (XLPE) [2].

XLPE features a low direct-current (DC) electrical conductivity σ_{DC} of about $10^{-14}\,\mathrm{S\,m^{-1}}$ at 70°C and an electric field of $20–30\,\mathrm{kV\,mm^{-1}}$ [3, 4]. Typically, peroxides are used for radical crosslinking of polyethylene, which however leads to the formation of byproducts such as methane, cumyl alcohol, acetophenone, or methylstyrene [5] that tend to compromise the dielectric properties of the insulation [6]. These byproducts must be removed via a time and energy intensive degassing step during cable production that involves heating of the extruded cable for a prolonged period of time [7]. As a result, considerable academic research efforts are currently dedicated to identifying alternative insulation materials that do not need to be crosslinked and instead remain thermoplastic [8].

Thermoplastic insulation materials that are being investigated comprise a higher-melting polyolefin such as high-density polyethylene (HDPE) [3, 9, 10] or a polypropylene (PP) based material [11–14]. PP-based insulation materials receive particular attention because of the high melting temperature of polypropylene resins of up to 170°C. The high stiffness of isotactic PP at low temperatures necessitates the use of copolymers or blends, resulting in formulations that are both sufficiently flexible and feature a high melting temperature. Two general approaches are being explored in the scientific literature: (i) the stiffness of PP is reduced through the incorporation of a rubbery phase, or (ii) LDPE is used as a base resin that is then reinforced by incorporation of a PP-rich phase [12–15].

PP-based formulations that have been considered include random [16, 17] and blocky propylene-ethylene copolymers [16] as well as random heterophasic propylene-ethylene copolymers [17]. For example, it has been reported that the incorporation of only 2% ethylene comonomer significantly improved the toughness of isotactic PP, which as a result could experience considerable tensile deformation [16, 17]. In addition, numerous blends have been investigated including binary blends of (i) isotactic PP with an ethylene-propylene copolymer [18–20], an ethylene-octene copolymer [20, 21] or a propylene-butylene copolymer [18], (ii) ternary blends of isotactic PP with an ethylene-octene and a propylene-ethylene copolymer [22–24], and (iii) binary blends of an ethylene-propylene copolymer with an ethylene-propylene rubber (EPR) [25] or a polystyrene-*b*-(ethylene-*co*-butylene)-*b*-polystyrene (SEBS) elastomer [26]. One intriguing example that has been explored is a ternary blend comprising isotactic PP, an ethylene-octene copolymer and a PP copolymer (with EPR inclusions), which resulted in a material with an elastic modulus of 10 MPa at 150°C and $\sigma_{DC} \approx 10^{-15}$ S m^{-1} at 80°C and an electric field of approximately 8 kV mm^{-1} [22].

Blending of LDPE and isotactic PP is complicated by their poor miscibility. The resulting phase-separated microstructure is characterized by weak domain interfaces that tend to compromise the thermo-mechanical properties of this type of formulation. As a result, thermoplastic insulation materials based on LDPE and PP have so far received lesser attention. Additives must be used that function as a compatibilizer or at least modify the interface between LDPE and PP domains. Recent work has shown that a small amount of SEBS, which is a common impact modifier for PP, can significantly improve the thermomechanical properties of PP:LDPE blends [27, 28]. Moreover, the addition of SEBS does not compromise the dielectric properties, resulting in ternary blends with an elastic modulus of 10 MPa at 150°C and a low $\sigma_{DC} \approx 2 \times 10^{-15}$ S m^{-1} at 70°C and 30 kV mm^{-1} [28]. A remaining challenge is the low elongation at break ε_{break} of this type of ternary blend, as pointed out by a recent review [14]. PP:LDPE:SEBS ternary blends were found to feature an $\varepsilon_{break} < 100\%$, in contrast to LDPE and SEBS which could be extended to 350% and 1400%, respectively [28].

The ductility of polyolefins is determined by the connectivity of the material, which is governed by the number of tie chains that connect crystal lamellae within spherulites as well as across the interface between spherulites [29]. In the case of PP, for example, the interface between spherulites tends to constitute a weak point [30] since impurities often concentrate in this region and voids can form [31–33]. Moreover, the number of tie chains that bridge the spherulite interface is important, which tends to decrease if the material is given sufficient time to crystallize [29]. As a result, rapidly cooled PP tends to be ductile, while prolonged annealing of PP can result in a brittle material [34].

Similar to neat PP, it can be anticipated that the mechanical response of PP:LDPE:SEBS ternary blends is significantly influenced by the crystallization conditions. Here, we exploit differences in the cooling rate to counter the previously observed brittleness of PP:LDPE:SEBS ternary blends and find that rapid cooling leads to a considerable increase in ductility. Gratifyingly, the cooling rate does not otherwise affect the promising electrical and thermomechanical properties, which allows to considerably enhance the scope of this promising type of thermoplastic insulation material.

2 | Experimental Section

2.1 | Materials

Isotactic PP with a melt flow index MFI = 3.3 g/10 min (230°C/2.16 kg), number-average molecular weight M_n = 46 kg mol^{-1}, polydispersity index PDI = 8.6 and isotacticity > 90%, LDPE with a MFI = 2 g/10 min (190°C/2.16 kg), M_n = 13 kg mol^{-1}, PDI = 9 and number of long-chain branches = 1.9 per 1000 carbons were provided by Borealis AB. SEBS with a MFI < 1 g/10 min (230°C/2.16 kg) and a polystyrene content of 18.5% to 22.5% was obtained from Kraton Corporation (Kraton G1642 HU).

2.2 | Sample Preparation

Materials were compounded in a Coperion ZSK 26 twin screw extruder at 150 rpm and 200°C, followed by extrusion and pelletization. Sheets with a thickness of 0.3, 1, or 4.5 mm were prepared by compression molding using a LabPro 200 Fontijne press. Samples were kept at 200°C for 5 min and then cooled at −10°C min^{-1} in the press or at about −130°C min^{-1} by placing films between cold steel plates, followed by conditioning at room temperature for 3 days prior to any measurements. Where specified, samples were then annealed for 24 h, followed by another 3 days of conditioning at room temperature.

2.3 | Differential Scanning Calorimetry

Measurements were carried out between −40°C and 200°C at a rate of 10°C min^{-1} using a DSC2 calorimeter from Mettler Toledo.

2.4 | Polarized Light Microscopy

Samples with a thickness of 10 μm were microtomed at −50°C using a PC PowerTome equipped with a glass knife. An Axio Scope A1 microscope from Zeiss was used in transmission mode with crossed polarizers.

2.5 | Tensile Deformation

Samples with shape type 5A were cut from 1 mm thick sheets according to ISO 527. An Instron 5565A instrument equipped with side-action pneumatic grips was used at a speed of $25\,mm\,min^{-1}$.

2.6 | Dynamic Mechanical Analysis

Rectangular samples with a width of 6 mm were cut from 1 mm thick sheets. Measurements were carried out with a TA Q800 DMA instrument in tensile mode between −50°C and 190°C, at a heating rate of $2°C\,min^{-1}$, a frequency of 1 Hz, and a maximum strain of 0.5%.

2.7 | Wide-Angle X-Ray Scattering

Diffractograms of 1 mm thick samples were recorded in reflection mode with a D8 Discover instrument from Bruker equipped with a CuK_α source (1.54 Å) and using a fixed slit mode (0.7 mm). To calculate the content of crystallographic forms, we deconvolve diffractograms using the WAXSFIT program [35].

2.8 | Small Angle X-Ray Scattering

Small angle x-ray scattering (SAXS) diffractograms were recorded with a Mat:Nordic instrument from SAXSLAB/Xenocs equipped with a microfocus CuK_α source (1.54 Å) and a Dectris Pilatus 300 K detector. Data were processed with the SAXSGui software.

2.9 | Thermal Conductivity Measurements

Four millimeter thick samples were analyzed with a TPS 2500S thermal constant analyzer from Hot Disk equipped with a Kapton sensor 5465 (radius = 3.189 mm) using a measurement time of 20 to 40 s and heating power of 20 to 25 mW. Prior to each measurement, samples were annealed for 2 h at the measurement temperature.

2.10 | DC Electrical Conductivity Measurements

The test cell consisted of a three-electrode system setup (measuring area diameter of Ø = 60 mm), placed in an oven at 70°C and connected to a Keithley 2290-10 high-voltage power supply. Before the measurement, a sample with a thickness of 0.3 mm was conditioned for 24 h at 70°C, and then a DC field of $30\,kV\,mm^{-1}$ was applied across the film for 24 h. The volume leakage current was recorded with a Keithley 6517B electrometer and dynamically averaged. The DC electrical conductivity was calculated based on the volume leakage current obtained at the end of the 24 h period.

3 | Results and Discussion

In a first set of experiments, we chose to compare tensile deformation of PP, LDPE and various binary and ternary blends (Table 1) cooled from the melt at $-10°C\,min^{-1}$. LDPE with a Young's modulus of $E = 167$ MPa is ductile and exhibits a strain at break $\varepsilon_{break} = 793\%$. In contrast, the selected isotactic PP grade with $E = 875$ MPa is considerably more brittle with ε_{break} of only 29% (Figure 1a and Table 2). Likewise, a binary blend of PP and LDPE comprising 56 wt% PP is found to be brittle with $\varepsilon_{break} = 11\%$ (Table 2 and Figure S1). We have previously observed that the same PP grade in LDPE forms a continuous phase for a PP content of 40 wt% or more [27]. Hence, we assign the brittleness of the PP:LDPE binary blend to poor connectivity within the continuous PP phase. We chose to compatibilize PP and LDPE with 20 wt% SEBS, which in a previous study resulted in a ternary blend that exhibited a promising combination of electrical and thermomechanical properties. The continuity of the PP phase is corroborated by the presence of more than 100 μm large spherulites, which can be discerned with polarized optical microscopy (Figure 1b). The ternary blend exhibited an intermediate ε_{break} with a median value of 239%, albeit with a considerable variation between samples (see Table 2), which necessitates further improvement of the ductility. Strikingly, both LDPE:SEBS and PP:SEBS binary blends exhibited a high ε_{break} (Table 2 and Figure S1), which indicates that the inclusion of the rubber phase does not introduce weak interfaces and that the here used PP grade can be highly ductile.

TABLE 1 | Composition of blends comprising PP, LDPE, and/or SEBS.

	wt% PP	wt% LDPE	wt% SEBS
PP	100	—	—
PP:LDPE	56	44	—
PP:SEBS	80	—	20
LDPE	—	100	—
LDPE:SEBS	—	80	20
PP:LDPE:SEBS	45	35	20

The ductility of PP is influenced by the type of crystal polymorphs that are present in the material. For instance, Tordjeman et al. have observed for β-nucleated isotactic PP that an increase in the β-phase content from 45% to 90% resulted in an increase in ε_{break} from 10% to 50% [36]. In another study, β-nucleation was found to increase ε_{break} from about 190% to 470%, provided that a high melt temperature of 240°C was selected [37]. We therefore employed wide-angle X-ray scattering (WAXS) to determine the amount of β phase according to: [38]

$$K_\beta = \frac{A(110)_\beta}{A(110)_\beta + A(110)_\alpha + A(040)_\alpha + A(130)_\alpha + A(117)_\gamma} \quad (1)$$

where $A(hkl)$ are the areas under the various diffraction peaks (see Figure 1c and Figure S2). For neat PP cooled at rate of $-10°C\,min^{-1}$ we obtain $K_\beta = 15\%$ with the remaining crystals mostly of α-phase type. The presence of β-phase crystals was confirmed by differential scanning calorimetry (DSC) heating thermograms, which feature two melting peaks at 150°C and 165°C (Table 3 and Figure S6) that can be assigned to melting of β- and α-crystals, respectively, which is likely accompanied by recrystallization [39]. Interestingly, PP:SEBS and PP:LDPE:SEBS blends did not feature an appreciable amount of β phase ($K_\beta < 1\%$) but nevertheless exhibited a higher degree

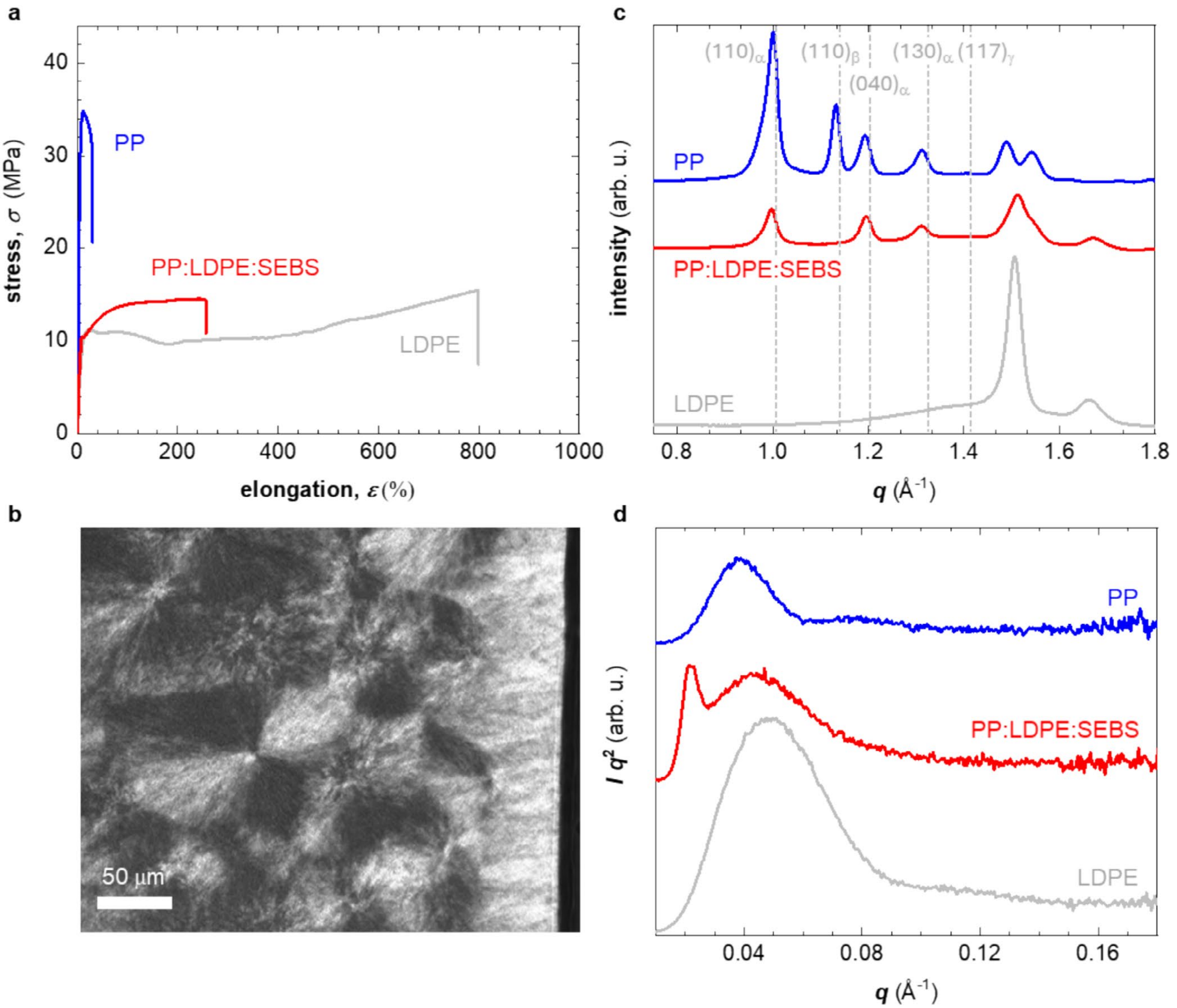

FIGURE 1 | (a) Representative stress–strain curves recorded during tensile deformation, (b) polarized optical micrograph of a 10 µm thin sheet of the SEBS:PP:LDPE ternary blend, (c) wide-angle X-ray scattering (WAXS) diffractograms, and (d) small-angle X-ray scattering (SAXS) Kratky plots of LDPE, PP, and SEBS:PP:LDPE cooled from the melt at $-10°C\,min^{-1}$. [Color figure can be viewed at wileyonlinelibrary.com]

TABLE 2 | Young's modulus E, stress and elongation at break, σ_{break} and ε_{break}, and storage modulus $E'_{150°C}$ at 150°C from DMA of PP, LDPE, and blends comprising PP, LDPE, and/or SEBS, prepared by cooling at $\Delta T/\Delta t = -10$ or $-130°C\,min^{-1}$; median values and standard deviations of five measurements.

	−10				−130			
$\Delta T/\Delta t$ (°C min^{-1})	E (MPa)	σ_{break} (MPa)	ε_{break} (%)	$E'_{150°C}$ (MPa)	E (MPa)	σ_{break} (MPa)	ε_{break} (%)	$E'_{150°C}$ (MPa)
PP	875 ± 63	35 ± 1	29 ± 4	144	734 ± 41	32 ± 2	998 ± 72	119
PP:LDPE	427 ± 39	21 ± 1	11 ± 2	35	345 ± 10	18 ± 1	15 ± 3	24
PP:SEBS	366 ± 11	41 ± 5	1012 ± 131	55	305 ± 15	40 ± 1	1226 ± 67	49
LDPE	167 ± 6	15 ± 1	793 ± 34	n.a.	150 ± 6	15 ± 1	824 ± 40	n.a.
LDPE:SEBS	74 ± 9	12 ± 2	872 ± 130	n.a.	70 ± 6	16 ± 1	1154 ± 43	n.a.
PP:LDPE:SEBS	227 ± 9	15 ± 2	239 ± 173	30	241 ± 17	24 ± 5	826 ± 172	33

of ductility compared to PP (Figure S1 and Table 2), suggesting that the amount of β-phase is not the cause for the observed brittleness of PP.

For samples cooled at a rate of $-10°C\,min^{-1}$, we also observed a maximum characteristic of the γ-crystallographic form of PP. The occurrence of a minor amount of the γ form in samples crystallized at atmospheric pressure has been observed previously [40]. We determined the amount of γ phase according to [38].

$$K_\gamma = \left(1 - K_\beta\right) \frac{A(117)_\gamma}{A(130)_\alpha + A(117)_\gamma} \tag{2}$$

For the here studied materials, K_γ is only 4% and since the presence of the γ phase does not strongly influence the ductility of PP [41], it is unlikely to be the reason for the brittleness of slowly cooled PP.

Small-angle X-ray scattering was used to obtain information about the long period L_p of the PP phase, which allowed to estimate the tie-chain probability for a polymer chain with molecular weight M according to the Huang–Brown model: [42]

$$P_M = \frac{1}{3}\left(1 - \frac{4b^3}{\sqrt{\pi}} \int_0^L r^2 e^{-b^2 r^2} dr\right) \tag{3}$$

where $b^2 = 3/2\overline{r}^2$ is related to the square of the end-to-end distance $\overline{r}^2 = Dnr_i^2$ of a random coil with a chain extension factor in the melt of $D=6.2$ [43], the number of links given by $n=M/(42\,g\,mol^{-1})$, and a link length of $r_i=2.52\,Å$. Both, SAXS Kratky plots of neat PP and PP:SEBS feature a diffraction peak at $q_p=0.38\,nm^{-1}$ (Figure 1d and Figure S3), which we assign to 1D stacking of crystalline lamellae and amorphous regions (the peak at $q=0.21\,nm^{-1}$ is assigned to hexagonally packed cylindrical PS domains in SEBS; Figure S4). We calculate a long period of $L_p = 2\pi/q_p$ of 16.5 nm, which allows to calculate the minimum distance L that a polymer chain needs to bridge in the amorphous phase according to:

$$L = L_p + L_c = L_p\left(1 + X_c \frac{\rho_s}{\rho_c}\right) \tag{4}$$

where L_c is the thickness of a crystalline lamellae and $X_c = \Delta H_m^{PP} / \Delta H_m^0$ is the mass crystallinity, ΔH_m^{PP} is the melting enthalpy of the PP fraction from DSC (Table 3), $\Delta H_m^0 = 209\,J\,g^{-1}$ is the enthalpy of fusion of PP [44, 45], ρ_s is the density of the sample and $\rho_c = 0.946\,g\,cm^{-3}$ is the density of the crystalline phase [46, 47]. Since brittle PP and ductile PP:SEBS have a similar ΔH_m^{PP} (Table 3), we obtain a comparable value of $P_M = 8\%$ and 9%, respectively, using $M = M_n$. Evidently, differences in tie-chain probability cannot explain the observed differences in ductility. Note that we were not able to estimate L_p of PP from SAXS in case of blends comprising both PP and LDPE because the lamellar stacking diffractions of the two polymers overlap (see Figure 1d and Figure S3).

Having concluded that the PP does not change connectivity in terms of tie-chain density, we instead turned our attention to the microstructure of PP domains and in particular the interface between spherulites. Optical microscopy suggests that voids are present at the interface between spherulites in PP cooled at $-10°C\,min^{-1}$, which constitute weak points in the material (Figure S5) [48]. We argue that voids form because of the increase in density upon crystallization, preventing the material from filling space as the growth fronts of spherulites meet. Moreover, the connectivity across spherulite boundaries can be influenced by the local tie chain density. Wang et al. have recently argued that the number of tie chains that bridge the spherulite interface decreases if the material is given time to crystallize [29].

It can be anticipated that rapid cooling is likely to result in (i) a lower crystallinity in case of PP, which would reduce the likelihood of void formation, and (ii) increase the number of tie chains that bridge the interface between spherulites. We therefore chose to rapidly solidify the here studied blend formulations, anticipating that a higher cooling rate may improve connectivity of the PP phase across spherulite boundaries. We observe that rapid cooling at $-130°C\,min^{-1}$ considerably increases the ductility of both PP and the PP:LDPE:SEBS ternary blend (Figure 2a), with an $\varepsilon_{break} = 1154\%$ and 826%, respectively (Table 2). Polarized optical microscopy of the ternary blend reveals more than 50 µm large spherulites, suggesting that the PP phase is again continuous (Figure 2b). In addition, we cannot discern voids at the interface between PP

TABLE 3 | Peak melting temperature of the LDPE and PP fraction, T_m^{PE} and T_m^{PP}, and melting enthalpy of the LDPE and PP fraction, ΔH_m^{PE} and ΔH_m^{PP}, of material cooled at $\Delta T/\Delta t = -10$ or $-130°C\,min^{-1}$, obtained from DSC first heating thermograms.

	−10				−130			
$\Delta T/\Delta t$ (°C min^{-1})	T_m^{PE} (°C)	ΔH_m^{PE} (J g^{-1})	T_m^{PP} (°C)	ΔH_m^{PP} (J g^{-1})	T_m^{PE} (°C)	ΔH_m^{PE} (J g^{-1})	T_m^{PP} (°C)	ΔH_m^{PP} (J g^{-1})
PP	—	—	150/165[a]	100	—	—	169	94
PP:LDPE	111	135	164	104	111	122	165	102
PP:SEBS	—	—	165	94	—	—	166	89
LDPE	112	130	—	—	111	124	—	—
LDPE:SEBS	112	117	—	—	112	110	—	—
PP:LDPE:SEBS	111	135	165	113	110	121	164	94

[a]Peak melting temperature of the β- and α-phase, respectively.

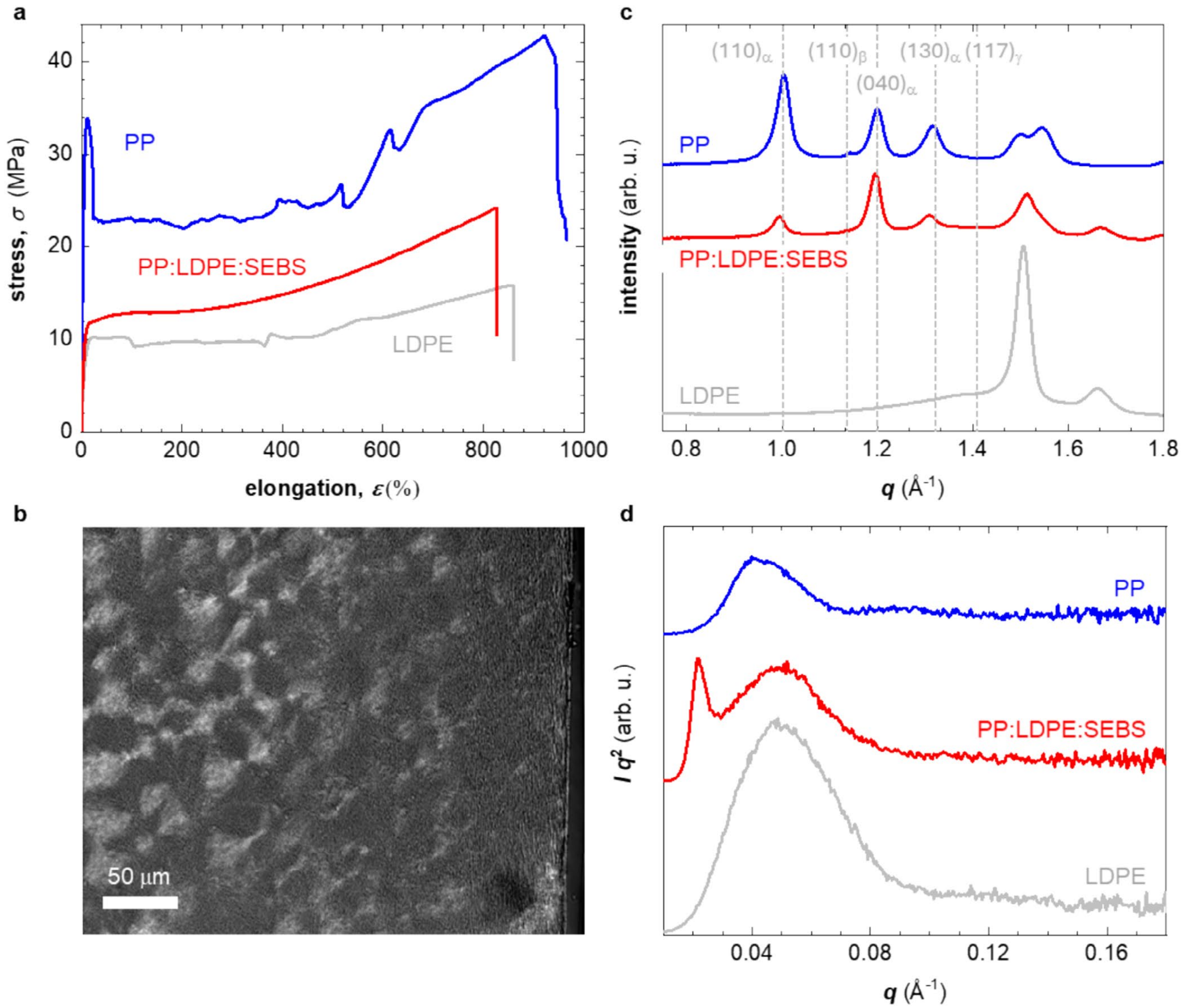

FIGURE 2 | (a) Stress–strain curves recorded during tensile deformation, (b) polarized optical micrograph of a 10 µm thin sheet of the SEBS:PP:LDPE ternary blend, (c) wide-angle X-ray scattering (WAXS) diffractograms, and (d) small-angle X-ray scattering (SAXS) Kratky plots of LDPE, PP, and SEBS:PP:LDPE rapidly cooled from the melt at −130°C min^{-1}. [Color figure can be viewed at wileyonlinelibrary.com]

spherulites, which we explain with the lower crystallinity of rapidly cooled material (cf. ΔH_m^{PP} in Table 3) and the smaller spherulite size.

DSC thermograms indicate that neither the crystallinity nor lamellar thickness of the LDPE and PP fraction drastically change upon increasing the cooling rate (cf. ΔH_m^{PE} and ΔH_m^{PP} as well as T_m^{PE} and T_m^{PP}; Table 3). WAXS diffractograms of both neat PP as well as various blends cooled at −130°C min^{-1} indicate that no significant amount of β phase is present (Figure 2c), in agreement with a study by Mollova et al., according to which despite the presence of a β-phase nucleating agent only the α-phase forms if isotactic PP is cooled at a rate of more than −100°C s^{-1} [49]. SAXS Kratky plots feature a distinct peak at $q_p = 0.40$ and 0.51 nm^{-1} in case of PP and PP:SEBS, respectively (Figure 2d), indicating a long period of $L_p = 15.7$ and 12.3 nm. We calculate a tie chain density of $P_M = 10\%$ for PP and 18% for PP:SEBS. The value that we obtain for neat PP cooled at −10°C min^{-1} and −130°C min^{-1} is comparable, suggesting that the pronounced difference in ductility does not arise due to differences in tie chain density within spherulites. Instead, the tie chain density of rapidly cooled PP:SEBS is significantly higher ($P_M = 18\%$) while it features a comparable ductility to slowly cooled material ($P_M = 9\%$) with an $\varepsilon_{\text{break}} > 1000\%$ in either case (Table 2). We thus argue that the high ductility of rapidly cooled material arises due to improved connectivity between PP spherulites due to (i) a reduction in the number of voids and (ii) a likely increase in the number of tie chains that bridge the spherulite interface, as proposed by Wang et al. [29].

The insulation of HVDC cables experiences elevated temperatures; at present an operating temperature of 70°C to 90°C is typical while even higher temperatures are possible during overload conditions such as lightning strikes and short circuits [2]. Therefore, we studied to which extent annealing for 24 h influences the ductility of PP, LDPE and the PP:LDPE:SEBS ternary blend. We observe that $\varepsilon_{\text{break}}$ of rapidly cooled material gradually decreases with the annealing temperature $T_{\text{annealing}}$,

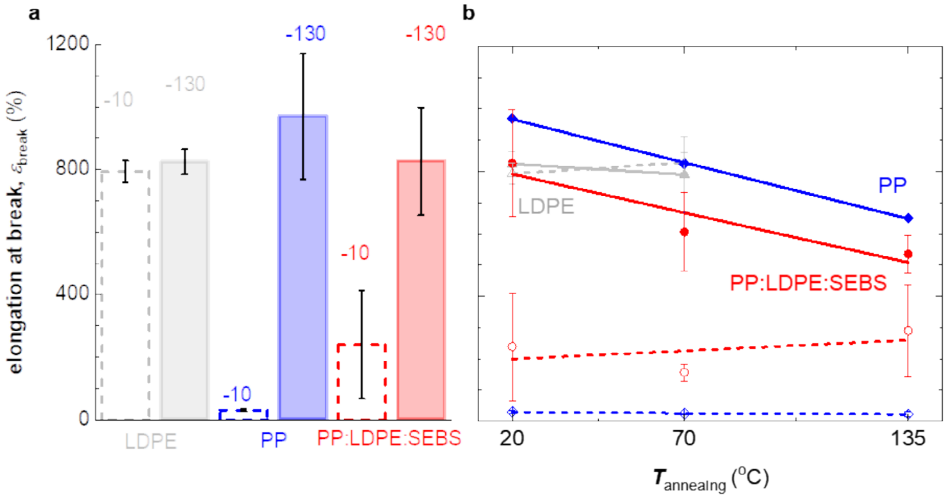

FIGURE 3 | Elongation at break ε_{break} of PP (blue), LDPE (gray) and the PP:LDPE:SEBS ternary blend (red) cooled slowly at −10°C min^{-1} (dashed lines) or rapidly at −130°C min^{-1} from the melt (solid lines) of (a) as-prepared samples and (b) annealed samples as a function of annealing temperature $T_{annealing}$ (samples were annealed for 24 h followed by conditioning for 3 days at room temperature; see Section 2). [Color figure can be viewed at wileyonlinelibrary.com]

while the ductility of slowly cooled material is less affected. Nevertheless, ε_{break} remains high with a value of about 650% in case of PP and 535% for PP:LDPE:SEBS (Figure 3). Upon annealing at 135°C, the degree of crystallinity of rapidly cooled PP increases from 45% to 53% (Figure S6 and Table S1), indicating that the material experienced secondary crystallization during annealing.

Dynamic mechanical analysis (DMA) was used to examine the impact of the cooling rate on the thermomechanical properties of ternary blends above the melting temperature of LDPE, $T_m^{PE} = 110°C$ (Table 3). DMA thermograms indicate that the cooling rate does not affect the elastic modulus E' of LDPE, PP and the PP:LDPE:SEBS ternary blend (Figure 4). The ternary blend maintains a value of $E' > 10$ MPa up to the melting temperature of PP, $T_m^{PE} = 164°C$ (Table 3) with a value of $E'_{150°C} = 33$ MPa at 150°C (see Table 2). Moreover, we note that the ternary blend displays a similar E' as LDPE below room temperature, while neat PP is significantly stiffer at low temperatures due to its comparatively high glass transition temperature $T_g \approx 0°C$ (Figure 4). Evidently, rapid cooling of the ternary blend allows to improve the ductility without otherwise influencing its advantageous thermomechanical properties.

In a final set of experiments, we carried out thermal and electric conductivity measurements to determine to which extent rapid cooling impacts the thermal and electrical behavior of the ternary blend. For PP, LDPE and all investigated binary and ternary blends we consistently observe that rapid cooling results in a slight reduction in thermal conductivity κ. For the ternary blend we find a reduction from $\kappa = 0.273$ to 0.268 W m^{-1} K^{-1} upon increasing the cooling rate from −10°C min^{-1} to −130°C min^{-1}, which we assign to a marginally lower crystallinity and/or lamellar thickness of both the PP and LDPE fraction in case of rapidly cooled material (cf. lower melting enthalpies ΔH_m^{PE} and ΔH_m^{PP} in Table 3). The thermal conductivity of the ternary blend lies in between

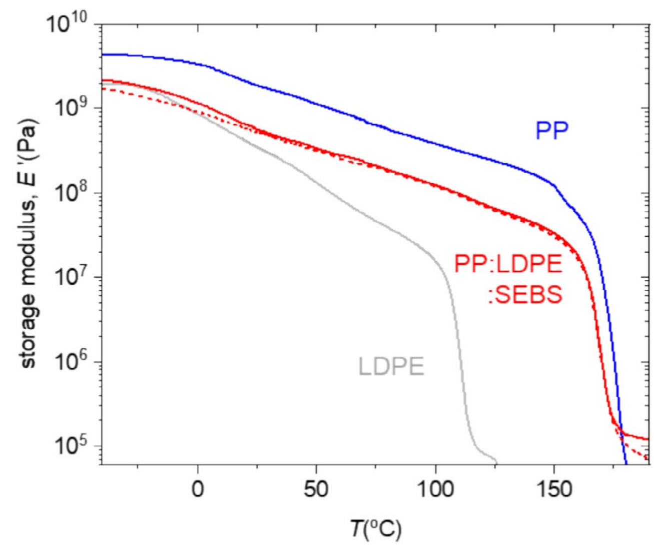

FIGURE 4 | Dynamic mechanical analysis (DMA) first heating thermograms of PP (blue), LDPE (gray) and the PP:LDPE:SEBS ternary blend (red) cooled slowly at −10°C min^{-1} (dashed lines) or rapidly at −130°C min^{-1} from the melt (solid lines). [Color figure can be viewed at wileyonlinelibrary.com]

values measured for PP with $\kappa \approx 0.25$ W m^{-1} K^{-1} and LDPE with $\kappa \approx 0.394$ W m^{-1} K^{-1}, as previously observed [28].

LDPE displayed an electrical conductivity $\sigma_{DC} = 18 \times 10^{-15}$ S m^{-1} (Table 4; see Figure S7 for recorded charging currents), when slowly cooled at −10°C min^{-1}, which is comparable to previously reported values [28]. Rapidly cooled PP and LDPE feature values of $\sigma_{DC} = 0.3$ and 13×10^{-15} S m^{-1}, respectively. The PP:LDPE:SEBS ternary blend featured a low electrical conductivity that was more comparable with the value determined for PP, with a similar $\sigma_{DC} = 0.8$ and 0.7×10^{-15} S m^{-1} for slowly and rapidly cooled material, respectively (Table 4). For ternary blends, additional measurements were performed for samples

TABLE 4 | Thermal conductivity κ at 25°C (mean and standard deviation of five measurements of one sample) and DC electrical conductivity σ_{DC} at 70°C and an electric field of 30 kV mm^{-1}.

	−10		−130	
$\Delta T / \Delta t$ (°C min^{-1})	κ (W m^{-1} K^{-1})	σ_{DC} (10^{-15} S m^{-1})	κ (W m^{-1} K^{-1})	σ_{DC} (10^{-15} S m^{-1})
PP	0.253 ± 0.001	n.m.	0.250 ± 0.001	0.3 ± 0.1[a]
PP:LDPE	0.287 ± 0.001	n.m.	0.284 ± 0.001	n.m.
PP:SEBS	0.237 ± 0.001	n.m.	0.222 ± 0.001	n.m.
LDPE	0.394 ± 0.002	18 ± 5[a]	0.386 ± 0.001	13 ± 4[a]
LDPE:SEBS	0.310 ± 0.001	26 ± 1[b]	0.299 ± 0.001	n.m.
PP:LDPE:SEBS	0.273 ± 0.001	0.8 ± 0.1[b]	0.268 ± 0.001	0.7 ± 0.2[a]

[a]single measurement and percentage error of 30% based on a comparison of five ternary blend samples [28].
[b]mean and max-min error of two measurements.

prepared with a cooling rate of −40°C min^{-1}, again yielding a similar $\sigma_{DC} = 0.5 \pm 0.1 \times 10^{-15}$ S m^{-1}. The invariance in σ_{DC} of the ternary blend agrees with a recent report by Zhan et al. who studied a heterophasic PP copolymer and observed that a change in cooling rate from -70°C min^{-1} to -1000°C min^{-1} resulted in a similar $\sigma_{DC} \approx 0.5 \times 10^{-15}$ S m^{-1} [50]. Evidently, the cooling rate can be altered without compromising the excellent electrical properties of the ternary blend.

4 | Conclusions

We have shown that the ductility of PP based insulation materials can be significantly improved by rapid cooling. The tensile deformation behavior of neat isotactic PP as well as a ternary blend comprising PP, LDPE, and SEBS can be drastically changed from brittle to highly ductile by increasing the cooling rate from the melt. Slow cooling at −10°C min^{-1} resulted in a ternary blend that displayed a highly varying ductility with samples varying from brittle to somewhat ductile and an average elongation at break $\varepsilon_{break} = 239\% \pm 173\%$. Instead, rapid cooling at −130°C min^{-1} resulted in a highly ductile material with a high $\varepsilon_{break} = 826\% \pm 172\%$, which maintained a high degree ductility even after prolonged annealing at temperatures up to at least 135°C. Otherwise, the ternary blend maintained its thermomechanical properties such as a relatively high elastic modulus above the melting temperature of LDPE. Moreover, no significant change in thermal and electrical conductivity was observed, indicating that the ductility of PP:LDPE:SEBS ternary blends can be improved without compromising its excellent thermomechanical and dielectric properties. Future work may entail theoretical studies such as molecular dynamics simulations that can deepen the understanding of the melt density [51] and tie chain formation [52], and kinetic Monte Carlo simulations that can provide knowledge about electrical transport in insulation materials [53].

Author Contributions

Christian Müller: conceptualization (equal), supervision (equal). **Przemyslaw Sowinski:** conceptualization (supporting), investigation (lead), methodology (lead). **Xiangdong Xu:** data curation (supporting), methodology (supporting). **Thomas Gkourmpis:** conceptualization (supporting), methodology (supporting). **Per-Ola Hagstrand:** conceptualization (equal), supervision (supporting).

Acknowledgments

The authors gratefully acknowledge financial support from Borealis. This project was in part performed at the Chalmers Materials Analysis Laboratory (CMAL).

Conflicts of Interest

The authors declare no conflicts of interest.

Data Availability Statement

The data that support the findings of this study are available from the authors upon reasonable request.

References

1. G. C. Montanari, P. H. F. Morshuis, M. Y. Zhou, et al., "Criteria Influencing the Selection and Design of HV and UHV DC Cables in New Network Applications," *High Voltage* 3, no. 2 (2018): 90–95, https://doi.org/10.1049/hve.2017.0098.

2. G. Mazzanti and M. Marzinotto, *Extruded Cables for High-Voltage Direct-Current Transmission: Advances in Research and Development* (Wiley, 2013).

3. M. G. Andersson, J. Hynynen, M. R. Andersson, et al., "Highly Insulating Polyethylene Blends for High-Voltage Direct-Current Power Cables," *ACS Macro Letters* 6, no. 2 (2017): 78–82, https://doi.org/10.1021/acsmacrolett.6b00941.

4. M. Mauri, A. I. Hofmann, D. Gómez-Heincke, et al., "Confinement-Enhanced Multi-Wavelength Photon Upconversion Based on Triplet-Triplet Annihilation in Nanostructured Glassy Polymers," *Advanced Science (Weinheim, Baden-Wurttemberg, Germany)* 69, no. 4 (2025): 404–412, https://doi.org/10.1002/pi.5966.

5. A. Smedberg, T. Hjertberg, and B. Gustafsson, "Crosslinking Reactions in an Unsaturated Low Density Polyethylene," *Polymer* 38, no. 16 (1997): 4127–4138, https://doi.org/10.1016/S0032-3861(96)00994-9.

6. H. Ren, L. Zhong, W. Zhao, et al., "Influence of Crosslinking By-products on DC Conductivity of HVDC XLPE Cable Insulation," in *2018 IEEE Conference on Electrical Insulation and Dielectric Phenomena (CEIDP)* (IEEE, 2018), 90–93, https://doi.org/10.1109/CEIDP.2018.8544909.

7. T. Andrews, R. N. Hampton, A. Smedberg, D. Wald, V. Waschk, and W. Weissenberg, "The Role of Degassing in XLPE Power Cable Manufacture," *IEEE Electrical Insulation Magazine* 22, no. 6 (2006): 5–16, https://doi.org/10.1109/Mei.2006.253416.

8. A. M. Pourrahimi, M. Mauri, S. D'Auria, R. Pinalli, and C. Müller, "Alternative Concepts for Extruded Power Cable Insulation: From Thermosets to Thermoplastics," *Advanced Materials (Deerfield Beach, Fla.)* 36, no. 52 (2024): 2313508, https://doi.org/10.1002/adma.202313508.

9. I. L. Hosier, A. S. Vaughan, and S. G. Swingler, "Structure–Property Relationships in Polyethylene Blends: The Effect of Morphology on Electrical Breakdown Strength," *Journal of Materials Science* 32, no. 17 (1997): 4523–4531, https://doi.org/10.1023/A:1018617200285.

10. I. L. Hosier, A. S. Vaughan, and S. G. Swingler, "On the Effects of Morphology and Molecular Composition on the Electrical Strength of Polyethylene Blends," *Journal of Polymer Science Part B: Polymer Physics* 38, no. 17 (2000): 2309–2322, https://doi.org/10.1002/1099-0488(20000901)38:17<2309::AID-POLB110>3.0.CO;2–7.

11. X. Huang, J. Zhang, P. Jiang, and T. Tanaka, "Material Progress Toward Recyclable Insulation of Power Cables Part 2: Polypropylene-Based Thermoplastic Materials," *IEEE Electrical Insulation Magazine* 36, no. 1 (2020): 8–18, https://doi.org/10.1109/MEI.2020.8932973.

12. T. Andritsch, A. Vaughan, and G. C. Stevens, "Novel Insulation Materials for High Voltage Cable Systems," *IEEE Electrical Insulation Magazine* 33, no. 4 (2017): 27–33, https://doi.org/10.1109/MEI.2017.7956630.

13. J. Li, K. Yang, K. Wu, Z. Jing, and J.-Y. Dong, "Eco-Friendly Polypropylene Power Cable Insulation: Present Status and Perspective," *IET Nanodielectrics* 6, no. 3 (2023): 130–146, https://doi.org/10.1049/nde2.12048.

14. G. Bánhegyi, "Compatibility Issues in High Voltage DC Cable Insulation Development," *Advanced Industrial and Engineering Polymer Research* 7, no. 4 (2024): 454–465, https://doi.org/10.1016/j.aiepr.2023.06.001.

15. A. Bjurström, H. Edin, H. Hillborg, et al., "A Review of Polyolefin-Insulation Materials in High Voltage Transmission; From Electronic Structures to Final Products," *Advanced Materials (Deerfield Beach, Fla.)* 36, no. 52 (2024): 2401464, https://doi.org/10.1002/adma.202401464.

16. X. Huang, Y. Fan, J. Zhang, and P. Jiang, "Polypropylene Based Thermoplastic Polymers for Potential Recyclable HVDC Cable Insulation Applications," *IEEE Transactions on Dielectrics and Electrical Insulation* 24, no. 3 (2017): 1446–1456, https://doi.org/10.1109/TDEI.2017.006230.

17. I. L. Hosier, L. Cozzarini, A. S. Vaughan, and S. G. Swingler, "Propylene Based Systems for High Voltage Cable Insulation Applications," *Journal of Physics: Conference Series* 183, no. 1 (2009): 012015, https://doi.org/10.1088/1742-6596/183/1/012015.

18. I. L. Hosier, A. S. Vaughan, and S. G. Swingler, "An Investigation of the Potential of Polypropylene and Its Blends for Use in Recyclable High Voltage Cable Insulation Systems," *Journal of Materials Science* 46, no. 11 (2011): 4058–4070, https://doi.org/10.1007/s10853-011-5335-9.

19. C. D. Green, A. S. Vaughan, G. C. Stevens, et al., "Thermoplastic Cable Insulation Comprising a Blend of Isotactic Polypropylene and a Propylene-Ethylene Copolymer," *IEEE Transactions on Dielectrics and Electrical Insulation* 22, no. 2 (2015): 639–648, https://doi.org/10.1109/TDEI.2015.7076758.

20. B. Dang, J. He, J. Hu, and Y. Zhou, "Large Improvement in Trap Level and Space Charge Distribution of Polypropylene by Enhancing the Crystalline – Amorphous Interface Effect in Blends," *Polymer International* 65, no. 4 (2016): 371–379, https://doi.org/10.1002/pi.5063.

21. Y. Zhou, J. He, J. Hu, X. Huang, and P. Jiang, "Evaluation of Polypropylene/Polyolefin Elastomer Blends for Potential Recyclable HVDC Cable Insulation Applications," *IEEE Transactions on Dielectrics and Electrical Insulation* 22, no. 2 (2015): 673–681, https://doi.org/10.1109/TDEI.2015.7076762.

22. D.-K. Kim, S. H. Lee, T. H. Kwon, et al., "Study on High-Temperature and High-Voltage Insulation Characteristics of Polypropylene Blend With Highly Packed Elastomeric Domains for Power Cable Applications," *Polymer Testing* 120 (2023): 107942, https://doi.org/10.1016/j.polymertesting.2023.107942.

23. S.-K. Hong, S. H. Lee, J. A. Han, et al., "Polypropylene-Based Soft Ternary Blends for Power Cable Insulation at Low-to-High Temperature," *Journal of Applied Polymer Science* 139, no. 6 (2022): 51619, https://doi.org/10.1002/app.51619.

24. S. Yu, S. H. Lee, J. A. Han, et al., "Insulative Ethylene-Propylene Copolymer-Nanostructured Polypropylene for High-Voltage Cable Insulation Applications," *Polymer* 202 (2020): 122674, https://doi.org/10.1016/j.polymer.2020.122674.

25. K. Yang, Y. Ren, K. Wu, et al., "Enhancing Electrical Properties of Impact Polypropylene Copolymer for Eco-Friendly Power Cable Insulation by Manipulating the Multiphase Structure Through Molten-State Annealing," *Composites Science and Technology* 223 (2022): 109422, https://doi.org/10.1016/j.compscitech.2022.109422.

26. Y. Liang, L. Weng, W. Zhang, and C. Li, "Block Polypropylene/Styrene-Ethylene-Butylene-Styrene Tri-Block Copolymer Blends for Recyclable HVDC Cable Insulation," *Materials Research Express* 7, no. 8 (2020): 085301, https://doi.org/10.1088/2053-1591/abab42.

27. Y. Ouyang, A. M. Pourrahimi, A. Lund, et al., "High-Temperature Creep Resistant Ternary Blends Based on Polyethylene and Polypropylene for Thermoplastic Power Cable Insulation," *Journal of Polymer Science* 59, no. 11 (2021): 1084–1094, https://doi.org/10.1002/pol.20210147.

28. Y. Ouyang, A. M. Pourrahimi, I. Östergren, et al., "Highly Insulating Thermoplastic Blends Comprising a Styrenic Copolymer for Direct-Current Power Cable Insulation," *High Voltage* 7, no. 2 (2022): 251–259, https://doi.org/10.1049/hve2.12177.

29. S.-Q. Wang, T. Smith, C. Gupta, and A. Y. Siavoshani, "Building a Phenomenological Chain-Level Understanding of Mechanics of Semicrystalline Polymers: 2. Conceptual," *Polymer* 274 (2023): 125877, https://doi.org/10.1016/j.polymer.2023.125877.

30. L. Barish, "The Study of Cracking and Fracturing of Spherulitic Isotactic Polypropylene," *Journal of Applied Polymer Science* 6, no. 24 (1962): 617–623, https://doi.org/10.1002/app.1962.070062403.

31. J. L. Way, J. R. Atkinson, and J. Nutting, "The Effect of Spherulite Size on the Fracture Morphology of Polypropylene," *Journal of Materials Science* 9, no. 2 (1974): 293–299, https://doi.org/10.1007/BF00550954.

32. K. Friedrich, "Strength and Fracture of Crystalline Isotactic Polypropylene and the Effect of Molecular and Morphological Parameters," in *Anwendungsbezogene Physikalische Charakterisierung Von Polymeren, Insbesondere Im Festen Zustand*, ed. E. W. Fischer, F. H. Müller, and R. Bonart (Steinkopff, 1979), 299–309.

33. G. C. Oppenlander, "Structure and Properties of Crystalline Polymers," *Science* 159, no. 3821 (1968): 1311–1319, https://doi.org/10.1126/science.159.3821.1311.

34. T. Smith, C. Gupta, A. Y. Siavoshani, and S.-Q. Wang, "Building a Phenomenological Chain-Level Understanding of Mechanics of Semicrystalline Polymers: 1. Experimental," *Polymer* 274 (2023): 125878, https://doi.org/10.1016/j.polymer.2023.125878.

35. M. Rabiej and S. Rabiej, "Application of the Artificial Neural Network for Identification of Polymers Based on Their X-Ray Diffraction Curves," *Computational Materials Science* 186 (2021): 110042, https://doi.org/10.1016/j.commatsci.2020.110042.

36. P. Tordjeman, C. Robert, G. Marin, and P. Gerard, "The Effect of α, β Crystalline Structure on the Mechanical Properties of Polypropylene," *European Physical Journal E: Soft Matter and Biological Physics* 4, no. 4 (2001): 459–465, https://doi.org/10.1007/s101890170101.

37. F. Luo, C. Geng, K. Wang, et al., "New Understanding in Tuning Toughness of β-Polypropylene: The Role of β-Nucleated Crystalline

Morphology," *Macromolecules* 42, no. 23 (2009): 9325–9331, https://doi.org/10.1021/ma901651f.

38. A. T. Jones, J. M. Aizlewood, and D. R. Beckett, "Crystalline Forms of Isotactic Polypropylene," *Makromolekulare Chemie* 75, no. 1 (1964): 134–158, https://doi.org/10.1002/macp.1964.020750113.

39. K. Zhu, Q. Ding, C. Hua, H. Fu, and J. Yao, "Effect of β-Nucleating Agent on Crystallization of Post-Consumer Polypropylene," *Thermochimica Acta* 675 (2019): 63–68, https://doi.org/10.1016/j.tca.2019.03.017.

40. P. Sowinski, S. Veluri, E. Piorkowska, K. Kwiecinski, S. A. E. Boyer, and J.-M. Haudin, "High-Pressure Crystallization of iPP Nanocomposites With Montmorillonite and Carbon Nanotubes," *Thermochimica Acta* 716 (2022): 179318, https://doi.org/10.1016/j.tca.2022.179318.

41. E. Lezak, Z. Bartczak, and A. Galeski, "Plastic Deformation of the γ Phase in Isotactic Polypropylene in Plane-Strain Compression," *Macromolecules* 39, no. 14 (2006): 4811–4819, https://doi.org/10.1021/ma0605907.

42. Y.-L. Huang and N. Brown, "Dependence of Slow Crack Growth in Polyethylene on Butyl Branch Density: Morphology and Theory," *Journal of Polymer Science Part B: Polymer Physics* 29, no. 1 (1991): 129–137, https://doi.org/10.1002/polb.1991.090290116.

43. L. J. Fetters, D. J. Lohse, C. A. García-Franco, P. Brant, and D. Richter, "Prediction of Melt State Poly(α-Olefin) Rheological Properties: The Unsuspected Role of the Average Molecular Weight per Backbone Bond," *Macromolecules* 35, no. 27 (2002): 10096–10101, https://doi.org/10.1021/ma025659z.

44. J. Brandrup, E. H. Immergut, E. A. Grulke, A. Abe, and D. R. Bloch, *Polymer Handbook* (Wiley, 1999).

45. B. Wunderlich, "CHAPTER VIII—Equilibrium Melting," in *Macromolecular Physics*, ed. B. Wunderlich (Academic Press, 1980), 1–127.

46. H. Awaya, "Morphology of Different Types of Isotactic Polypropylene Spherulites Crystallized From Melt," *Polymer* 29, no. 4 (1988): 591–596, https://doi.org/10.1016/0032-3861(88)90071-7.

47. A. Rozanski, M. Safandowska, and A. Krajenta, "DSC/SAXS Analysis of the Thickness of Lamellae of Semicrystalline Polymers-Restrictions in the Case of Materials With Swollen Amorphous Phase," *Polymer Testing* 65 (2018): 189–196, https://doi.org/10.1016/j.polymertesting.2017.11.028.

48. A. Gałeski and E. Piórkowska, "Localized Volume Deficiencies as an Effect of Spherulite Growth. II. The Three-Dimensional Case," *Journal of Polymer Science: Polymer Physics Edition* 21, no. 8 (1983): 1313–1322, https://doi.org/10.1002/pol.1983.180210804.

49. A. Mollova, R. Androsch, D. Mileva, M. Gahleitner, and S. S. Funari, "Crystallization of Isotactic Polypropylene Containing Beta-Phase Nucleating Agent at Rapid Cooling," *European Polymer Journal* 49, no. 5 (2013): 1057–1065, https://doi.org/10.1016/j.eurpolymj.2013.01.015.

50. Y. Zhan, S. Hou, B. Hui, et al., "Effects of Processing Method on the Structure and Electrical Performance of Polypropylene Containing Intrinsic Elastomers for Cable Insulation Applications," *Journal of Polymer Research* 31, no. 2 (2024): 37, https://doi.org/10.1007/s10965-024-03876-x.

51. A. S. Jawed, M. N. Khan, N. A. Khan, M. A. Hakeem, and P. Khan, "Thermodynamic Insights Into Variation in Thermomechanical and Physical Properties of Isotactic Polypropylene: Effect of Shear and Cooling Rates," *ACS Omega* 8, no. 40 (2023): 36775–36788, https://doi.org/10.1021/acsomega.3c03378.

52. F. Nilsson, X. Lan, T. Gkourmpis, M. S. Hedenqvist, and U. W. Gedde, "Modelling Tie Chains and Trapped Entanglements in Polyethylene," *Polymer* 53, no. 16 (2012): 3594–3601, https://doi.org/10.1016/j.polymer.2012.05.045.

53. M. Unge, H. Aspåker, F. Nilsson, M. Pierre, and M. S. Hedenqvist, "Coarse-Grained Model for Prediction of Hole Mobility in Polyethylene," *Journal of Chemical Theory and Computation* 19, no. 21 (2023): 7882–7894, https://doi.org/10.1021/acs.jctc.3c00210.

Supporting Information

Additional supporting information can be found online in the Supporting Information section.